chemistry

Article

The Anion Impact on Dimensionality of Cadmium(II) Complexes with Nicotinamide

Željka Soldin [1,*], Boris-Marko Kukovec [2,*], Milica Kovačić [3], Marijana Đaković [1] and Zora Popović [1]

[1] Division of General and Inorganic Chemistry, Department of Chemistry, Faculty of Science, University of Zagreb, Horvatovac 102a, HR-10000 Zagreb, Croatia; mdjakovic@chem.pmf.hr (M.Đ.); zpopovic@chem.pmf.hr (Z.P.)
[2] Department of Physical Chemistry, Faculty of Chemistry and Technology, University of Split, Ruđera Boškovića 35, HR-21000 Split, Croatia
[3] Institute for Medical Research and Occupational Health, Ksaverska Cesta 2, HR-10000 Zagreb, Croatia; mkovacic@imi.hr
* Correspondence: zeljka.chem@pmf.hr (Ž.S.); bmkukovec@ktf-split.hr (B.-M.K.)

Abstract: Three novel cadmium(II) coordination compounds, the dimeric $[Cd(CH_3COO)_2(nia)_2]_2$ (**1**), the polymeric $\{[Cd(nia)_4](ClO_4)_2\}_n$ (**2**), and the monomeric $[Cd(H_2O)_3(nia)_3](ClO_4)_2\cdot nia$ (**3**), were prepared in the reactions of the nicotinamide (pyridine-3-carboxamide, nia) with the corresponding cadmium(II) salts. All prepared compounds were characterized by elemental analyses, FT-IR spectroscopy, TGA/DTA, and single crystal X-ray analysis. The impact of anions (acetate, perchlorate) and solvent used on the dimensionality of cadmium(II) complexes and the cadmium(II) coordination environment was investigated. The bridging capabilities of acetate ions enabled the formation of dimers in the crystal structure of **1**. It was shown that the dimensionality of perchlorate complexes depends on the solvent used. The coordination polymer **2** is isolated from an ethanol solution, while monomeric compound **3** was obtained by using a water/ethanol mixture as a solvent. The pentagonal-bipyramidal coordination of cadmium(II) was found in the presence of chelating and bridging acetate ions in **1**. In the presence of non-coordinating perchlorate anions in **2** and **3**, the coordination geometry of cadmium(II) is found to be octahedral. The supramolecular amide-amide homosynthon $R_2^2(8)$ was preserved in the hydrogen-bonded frameworks of all three compounds.

Keywords: cadmium(II); nicotinamide; perchlorate; acetate; dinuclear complex; coordination polymer; mononuclear complex; amide-amide homosynthon

check for updates

Citation: Soldin, Ž.; Kukovec, B.-M.; Kovačić, M.; Đaković, M.; Popović, Z. The Anion Impact on Dimensionality of Cadmium(II) Complexes with Nicotinamide. *Chemistry* **2023**, *5*, 1357–1368. https://doi.org/10.3390/chemistry5020092

Academic Editors: Zoi Lada and Konstantis Konidaris

Received: 5 April 2023
Revised: 18 May 2023
Accepted: 19 May 2023
Published: 1 June 2023

1. Introduction

The cadmium(II) coordination compounds have been of great interest for some time, particularly in the area of luminescent materials [1–6]. The ability of cadmium(II) to adopt different coordination geometries, such as tetrahedral, trigonal bypiramidal, octahedral, and pentagonal bipyramidal, allows the construction of different architectures and can be used as a powerful crystal engineering tool. Such flexible coordination geometry of the colorless cadmium(II) ion enables the formation of coordination compounds with diverse structural features and promising luminescence properties. Fine tuning of desired physical properties by impacting on the crystal structure is possible through the employment of multi-functional ligands, such as pyridine-amide-based ligands. It is well known that such ligands have the ability to self-assemble through the combination of covalent bonds with metal ions and the establishment of robust supramolecular synthons via hydrogen bonds [6–10]. The assembly of organic ligands into metal-organic structures could produce multifunctional luminescent materials [1,2]. In addition, a systematic study of metal-organic structures with different anions enables a better understanding of the influence of counter ions with different coordination and hydrogen-bonding abilities on the supramolecular assembly [10–14].

Previously, we tuned the zinc(II) coordination environment in the zinc(II) coordination compounds with isonicotinamide (pyridine-4-carboxamide, isn) by selecting anions with different coordination abilities: simple halide anions (chloride, bromide), bulky perchlorate anion, and multiple *O*-donor atom anions (nitrate and acetate) with a high potential for chelating or bridging the zinc(II) ions. The zinc(II) ion was found to be low-coordinated (tetrahedral) in the presence of chloride or bromide anions, but its coordination environment was enlarged to the octahedral or pentacoordinated in the presence of either perchlorate, nitrate, or acetate anions [11]. Furthermore, we have shown that the introduced anions (excluding perchlorate) do not significantly affect the supramolecular features of the prepared zinc(II) coordination compounds with isonicotinamide, as the centrosymmetric amide-amide supramolecular homosynthon (a $R_2^2(8)$ hydrogen-bonded ring motif, Scheme 1) remained preserved in the presence of halide, nitrate, and acetate anions. However, the said homosynthon was disrupted in the presence of the perchlorate anions [11].

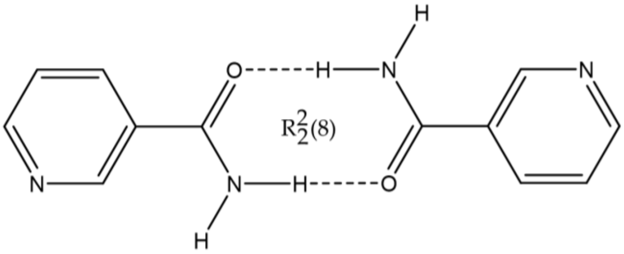

Scheme 1. The amide-amide $R_2^2(8)$ supramolecular synthon.

In this study, we wanted to check if the cadmium(II) coordination environment and the dimensionality of the corresponding compound can be tuned as well by employing anions with different coordination abilities: a chelating and bridging acetate or a bulky perchlorate, which are not expected to coordinate. Similarly to the zinc(II) ion, the cadmium(II) coordination environment is even more unpredictable due to the absence of the crystal field splitting stabilization. Hence, the cadmium(II) environment is mostly influenced by the cadmium(II) radius and by the donor atoms available for coordination, resulting in even higher coordination numbers, e.g., seven. This time, nicotinamide (nia) was used in the design of cadmium(II) coordination compounds in the hope that it would act similarly to isonicotinamide—coordinating to a cadmium(II) ion monodentately via its pyridine N atom, with the uncoordinated amide group participating in the expected amide-amide homosynthon $R_2^2(8)$. Finally, we wanted to check the robustness of the said homosynthon by introducing acetate or perchlorate ions, both containing O acceptor atoms capable of competing for the amide protons, in the corresponding crystal packings.

2. Materials and Methods

2.1. Materials and Physical Measurements

All commercially available chemicals were of reagent grade and were used as received without further purification. CHN elemental analyses were carried out with a Perkin-Elmer 2400 Series II CHNS analyzer in Analytical Services Laboratories of the Ruđer Bošković Institute, Zagreb, Croatia.

The IR spectra were obtained from KBr pellets in the range 4400–450 cm^{-1} on a Perkin-Elmer Spectrum Two FT-IR spectrometer.

Thermogravimetric analysis was performed using a simultaneous TGA-DTA analyzer (Mettler-Toledo TGA/SDTA 851e). The samples were placed in aluminum pans (40 µL) and heated in flowing nitrogen (50 mL min^{-1}) from room temperature up to 500 °C at a rate of 5 °C min^{-1}. Data collection and analysis were performed using the program package STARe Software 16.40 MettlerToledo GmbH.

2.2. Syntheses of the Compounds

2.2.1. Synthesis of $[Cd(CH_3COO)_2(nia)_2]_2$ (**1**)

A solution of nia (0.33 g, 2.7 mmol) in 5 mL H_2O was added dropwise to a solution of $Cd(CH_3COO)_2{\cdot}2H_2O$ (0.30 g, 1.3 mmol) in 5 mL H_2O and stirred for 30 min. After three weeks, 10 mL of EtOH was added to the reaction mixture. The colorless crystals were filtered off after a few days, washed with EtOH, and dried in air. Yield: 76% (based on $Cd(CH_3COO)_2{\cdot}2H_2O$). *Anal.* Calc. for $Cd_2C_{32}H_{36}N_8O_{12}$: C, 40.48; H, 3.82; N, 11.80. Found: C, 40.49; H, 4.19; N, 11.67.

IR (KBr disc, cm^{-1}): 3407(s, br), 3321(s, br), 3264(s, br), 3195(s, br), 1696(s), 1670(vs), 1621(s), 1580(vs), 1411(s), 1342(w), 1200(w), 1140(w), 1048(w), 1028(vw), 931(vw), 825(vw), 792(w), 694(m), 649(m), 626(m), 568(w).

2.2.2. Synthesis of $\{[Cd(nia)_4](ClO_4)_2\}_n$ (**2**)

A solution of nia (0.24 g, 2 mmol) in 5 mL EtOH was added dropwise to a solution of $Cd(ClO_4)_2{\cdot}H_2O$ (0.30 g, 0.9 mmol) in 5 mL EtOH and stirred for 30 min. After three days, colorless crystals were obtained, filtered off, washed with EtOH, and dried in air. Yield: 82% (based on $Cd(ClO_4)_2{\cdot}H_2O$). *Anal.* Calc. for $CdCl_2C_{24}H_{24}N_8O_{12}$: C, 36.04; H, 3.02; N, 14.01. Found: C, 36.56; H, 2.89; N, 14.33.

IR (KBr disc, cm^{-1}): 3408(m, br), 3314(m, br), 3263(w, br), 3187(m, br), 1666(vs), 1622(s), 1600(m), 1579(w), 1479(vw), 1443(w), 1398(m), 1200(w), 1143(vs), 1113(vs), 1086(vs), 1047(w), 940(vw), 824(vw), 793(w), 753(vw), 694(m), 648(w), 628(m), 562(w).

2.2.3. Synthesis of $[Cd(H_2O)_3(nia)_3](ClO_4)_2{\cdot}nia$ (**3**)

A solution of nia (0.24 g, 2 mmol) in 5 mL H_2O was added dropwise to a solution of $Cd(ClO_4)_2{\cdot}H_2O$ (0.30 g, 0.9 mmol) in 10 mL H_2O and stirred for 30 min. After three weeks, 10 mL of EtOH was added to the reaction mixture. The colorless crystals were filtered off after a few days, washed with EtOH, and dried in air. Yield: 70% (based on $Cd(ClO_4)_2{\cdot}H_2O$). *Anal.* Calc. for $CdCl_2C_{24}H_{30}N_8O_{15}$: C, 33.76; H, 3.54; N, 13.12. Found: C, 33.89; H, 3.71; N, 13.47.

IR (KBr disc, cm^{-1}): 3358(s, br), 3193(s, br), 1695(vs), 1664(vs), 1624(s), 1599(s), 1576(m), 1402(s), 1201(m), 1094(vs, br), 935(vw), 834(vw), 793(w), 764(w), 695(m), 624(s), 628(m).

2.3. X-ray Crystallographic Analysis

The suitable single crystals of **1–3** were selected and mounted onto thin glass fibers. The data collection was carried out on an Oxford Diffraction Xcalibur four-circle kappa geometry diffractometer with Xcalibur Sapphire 3 CCD detector, using graphite monochromated MoKα (λ = 0.71073 Å) radiation at room temperature (296(2) K) and by applying the CrysAlisPro Software system [15]. The data reduction and cell refinement were performed by the CrysAlisPro Software system [15]. The structures were solved by SHELXT [16] and refined by SHELXL [17]. The refinement procedure was performed by full-matrix least-squares methods based on F^2 values against all reflections. The figures were made with MERCURY (Version 2022.3.0) [18]. The crystallographic data for **1–3** are summarized in Table 1.

Table 1. The crystallographic data for $[Cd(CH_3COO)_2(nia)_2]_2$ (**1**), $\{[Cd(nia)_4](ClO_4)_2\}_n$ (**2**), and $[Cd(H_2O)_3(nia)_3](ClO_4)_2{\cdot}nia$ (**3**).

Compound	**1**	**2**	**3**
Formula	$C_{32}H_{36}Cd_2N_8O_{12}$	$C_{24}H_{24}CdCl_2N_8O_{12}$	$C_{24}H_{30}CdCl_2N_8O_{15}$
M_r	949.51	799.81	853.86
Crystal system, space group	monoclinic, $P2_1/n$ (No. 14)	monoclinic, $P2_1/c$ (No. 14)	monoclinic, $P2_1/n$ (No. 14)
a (Å)	11.2351(2)	7.55240(10)	7.4629(2)
b (Å)	14.8801(2)	12.9826(2)	24.0425(6)

Table 1. *Cont.*

Compound	1	2	3
c (Å)	12.5650(3)	16.0880(2)	18.6052(4)
β (°)	103.108(2)	92.2960(10)	92.373(2)
V (Å^3)	2045.88(7)	1576.16(4)	3335.41(14)
Z	2	2	4
D_{calc} (g cm^{-3})	1.541	1.685	1.700
μ (mm^{-1})	1.104	0.936	0.896
R [$I \geq 2\sigma(I)$]	0.0485	0.0331	0.0344
wR [all data]	0.1714	0.0956	0.1002

3. Results

3.1. Synthesis

Compounds **1**–**3** were prepared from ethanol or water/ethanol solutions by reactions of nia with the corresponding cadmium(II) salts using two different ligand-to-metal ratios, 1:1 and 2:1 (Scheme 2). Regardless of the ratio used, the same type of compounds was always obtained. The reactions using 2:1 stoichiometry resulted in higher yields. Depending on the solvent used, two types of perchlorate compounds were prepared.

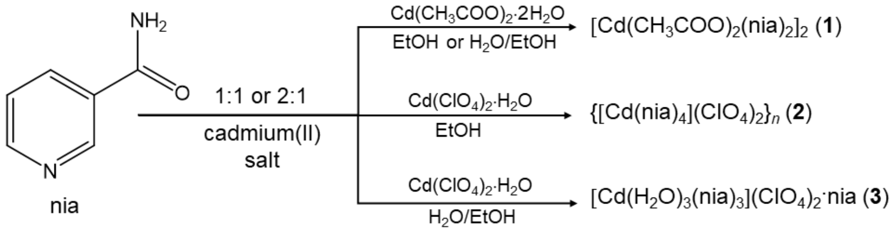

Scheme 2. Preparation of $[Cd(CH_3COO)_2(nia)_2]_2$ (**1**), $\{[Cd(nia)_4](ClO_4)_2\}_n$ (**2**), and $[Cd(H_2O)_3(nia)_3](ClO_4)_2\cdot$nia (**3**).

The dimeric coordination compound **1** was obtained from ethanol or water/ethanol solutions. Single crystals of compound **1** were obtained by adding ethanol to an aqueous reaction mixture. The perchlorate polymeric (**2**) and monomeric (**3**) compounds were obtained in the reactions of the nia with cadmium(II) perchlorate monohydrate. The coordination polymer **2** was obtained from an ethanol solution, while monomeric compound **3** was prepared from a water/ethanol solution. Compound's **3** solubility in water was decreased by the addition of ethanol to the reaction mixture, which led to the crystallization of the product.

3.2. Crystal Structures

The asymmetric unit of $[Cd(CH_3COO)_2(nia)_2]_2$ (**1**) is composed of a cadmium(II) ion, two coordinated acetate ions, and two coordinated nicotinamide molecules (Figure 1a). The cadmium(II) ion is heptacoordinated with the O3 and O4 atoms (from an *O,O′*-chelating acetate ion), the O5, O6, and O5^{i} atoms (from two *O,O′*-chelating and bridging acetate ions) in the equatorial plane, whilst the pyridine N1 and N3 atoms (from two separate *N*-monodentate nicotinamide ligands) are placed in the axial positions (a symmetry code (i): $-x + 1, -y + 2, -z$). The cadmium(II) coordination environment can be best described as a distorted pentagonal bipyramid (N3–Cd1–N1, 179.0(1)°; Figure 1a, Table S1). The symmetry-related cadmium(II) ions are bridged with two acetate ions into a centrosymmetric dimer of **1**, resulting in two types of acetate ions: two of them are *O,O′*-chelating only (via O3 and O4 atoms), whilst two acetate ions are both *O,O′*-chelating (via O5 and O6 atoms) and bridging (the O5 atom is bound to both symmetry-related cadmium(II) ions). The cadmium(II) coordination environment is highly distorted, as suggested by the bond angle values (Table S1); such a distortion is caused by the *O,O′*-bidentate binding of the acetate ions (the bite angles O4–Cd1–O3 (53.8(1)°) and O5–Cd1–O6 (123.9(3)°)). As a consequence, the four-membered chelate rings Cd1/O3/C13/O4, Cd1/O5/C15/O6, and Cd1/O5/Cd1^{i}/O5^{i} were formed within the dimer of **1**. The cadmium(II) complexes with acetate and either picolinamide, nicotinamide, or isonicotinamide are not known from the literature [19]. However, a similar zinc(II) complex with acetate and isonicotinamide is known, also being a dimer connected via three bridging acetate ions [11]. As opposed to **1**, there are three different coordination modes of acetate: two acetate anions are bridging (each O atom is bound to a separate Zn(II) ion), the third acetate is chelating (as in **1**), and the fourth one is both chelating and bridging (as in **1**). One of the zinc(II) ions in the dimer is octahedral, while the other is pentacoordinated [11].

The asymmetric unit of $\{[Cd(nia)_4](ClO_4)_2\}_n$ (**2**) consists of a cadmium(II) ion lying in an inversion center, two coordinated nicotinamide molecules, and an uncoordinated perchlorate ion (Figure 1b). The cadmium(II) ion is octahedrally coordinated with the pyridine N1 and N1^{ii} atoms (from two *N*,*O*′-bridging nicotinamide ligands; a symmetry code (ii): $-x + 1, -y, -z$), with the pyridine N3 and N3^{ii} atoms (from two terminal *N*-monodentate nicotinamide ligands), and with the amide O1 and O1^{ii} atoms (from two *N*,*O*′-bridging nicotinamide ligands) in the *trans* position (O1–Cd1–O1^{ii}, 180°; Figure 1b, Table S1). The octahedral cadmium(II) coordination environment is slightly distorted, as evidenced by the bond angle values (Table S1). The adjacent cadmium(II) ions in **2** are connected by two antiparallel *N*,*O*′-bridging nicotinamide ligands, resulting in an infinite 1-D polymeric chain along the *a* crystallographic axis (Figure 2). There are two types of nicotinamide ligands in **2**: *N*,*O*′-bridging (via the pyridine N1 and amide O1 atoms) and terminal *N*-monodentate (via the pyridine N3 atom). Consequently, centrosymmetric twelve-membered macrocyclic rings are formed within the 1-D polymeric chain of **2** (Figure 2). There are no similar polymeric cadmium(II) complexes with either picolinamide, nicotinamide, or isonicotinamide in the literature. However, two dimeric cadmium(II) complexes with the same antiparallel *N*,*O*′-bridging of nicotinamide are known [20,21].

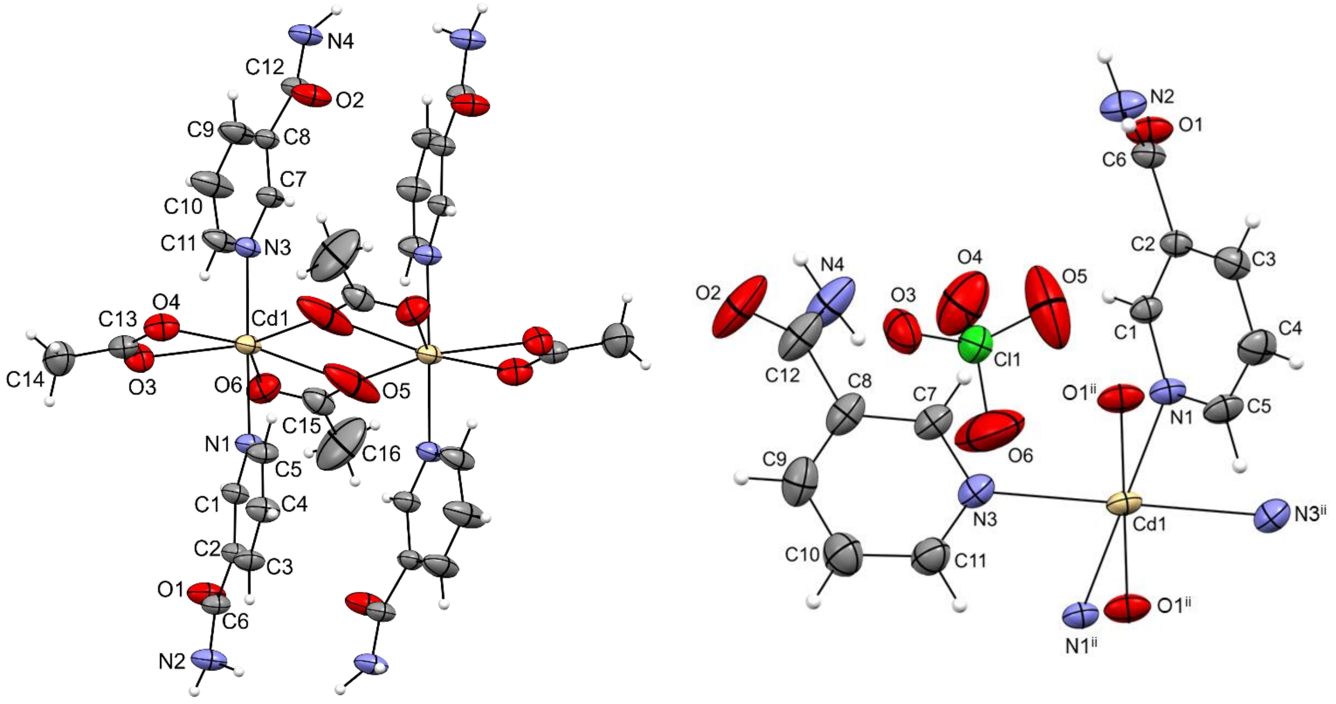

(**a**) (**b**)

Figure 1. *Cont.*

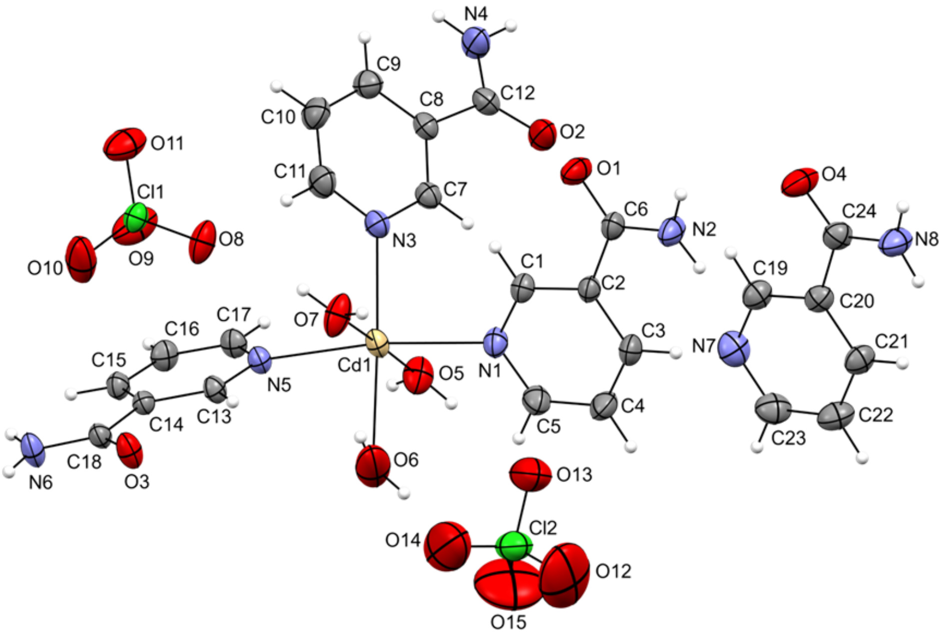

(**c**)

Figure 1. ORTEP-style plots of $[Cd(CH_3COO)_2(nia)_2]_2$ (**1**) (**a**), $\{[Cd(nia)_4](ClO_4)_2\}_n$ (**2**) (**b**), and $[Cd(H_2O)_3(nia)_3](ClO_4)_2 \cdot nia$ (**3**) (**c**), with the atomic numbering schemes. The thermal ellipsoids are drawn at the 40% probability level at 296(2) K, and hydrogen atoms are shown as spheres of arbitrary radii (symmetry code (ii): $-x + 1$, $-y$, $-z$).

The asymmetric unit of $[Cd(H_2O)_3(nia)_3](ClO_4)_2 \cdot nia$ (**3**) consists of a cadmium(II) ion, three coordinated water molecules, three coordinated nicotinamide molecules, two uncoordinated perchlorate ions, and a cocrystallized nicotinamide molecule (Figure 1c). The cadmium(II) ion is octahedrally coordinated with three water molecules (the O5, O6, and O7 atoms) and three pyridine N1, N3, and N5 atoms (from three separate *N*-monodentate nicotinamide ligands), resulting in a *mer*-isomer (Figure 1c). The octahedral cadmium(II) coordination environment is only slightly distorted (Table S1). The *N*-monodentate coordination mode of nicotinamide (via the pyridine N atom) can be frequently found in the corresponding cadmium(II) complexes [5,22–31]. Similarly to **3**, there are also cocrystallized nicotinamide molecules in the crystal packing of a cadmium(II) complex with nicotinamide and nitrate anions [32].

There are strong intermolecular N–H$\cdots$O and weak C–H$\cdots$O hydrogen bonds observed in all the structures of **1**–**3**, while the O–H$\cdots$O and O–H$\cdots$N hydrogen bonds are present only in the structure of **3** (Table S2). The centrosymmetric dimers of **1** are connected into a double chain via the respective amide groups, resulting in the formation of the dimeric amide-amide $R_2^2(8)$ hydrogen-bond motif within the chain. These chains are in turn assembled by N_{amide}–H$\cdots$$O_{acetate}$ hydrogen bonds into a hydrogen-bonded framework (Figure 3). The 1-D polymeric chains in **2** are linked into a network (parallel to the (0 0 1) plane) via the amide groups, giving rise to the hydrogen-bond $R_2^2(8)$ motif within the network. These networks are in turn assembled by the N_{amide}–H$\cdots$$O_{perchlorate}$ hydrogen bonds along the *c* crystallographic axis, forming a hydrogen-bonded framework (Figure 4). The perchlorate ions are placed between these networks, being connected to the amide groups from the surrounding networks by N_{amide}–H$\cdots$$O_{perchlorate}$ hydrogen bonds (forming the dimeric hydrogen-bond $R_1^2(5)$ motif between an amide group and a perchlorate ion) and, thus, additionally stabilizing the said framework. The $[Cd(H_2O)_3(nia)_3]$ molecules, perchlorate ions, and cocrystallized nicotinamide molecules are assembled by the said hydrogen bonds (Table S2) into a complex hydrogen-bonded framework of **3**. The most notable hydrogen-bond motifs found within this framework are the already mentioned dimeric $R_2^2(8)$ and $R_1^2(5)$ motifs, but also the tetrameric $R_4^4(16)$ motif, formed between two [Cd(H_2O)$_3$(nia)$_3$] molecules and two perchlorate ions (Figure 5).

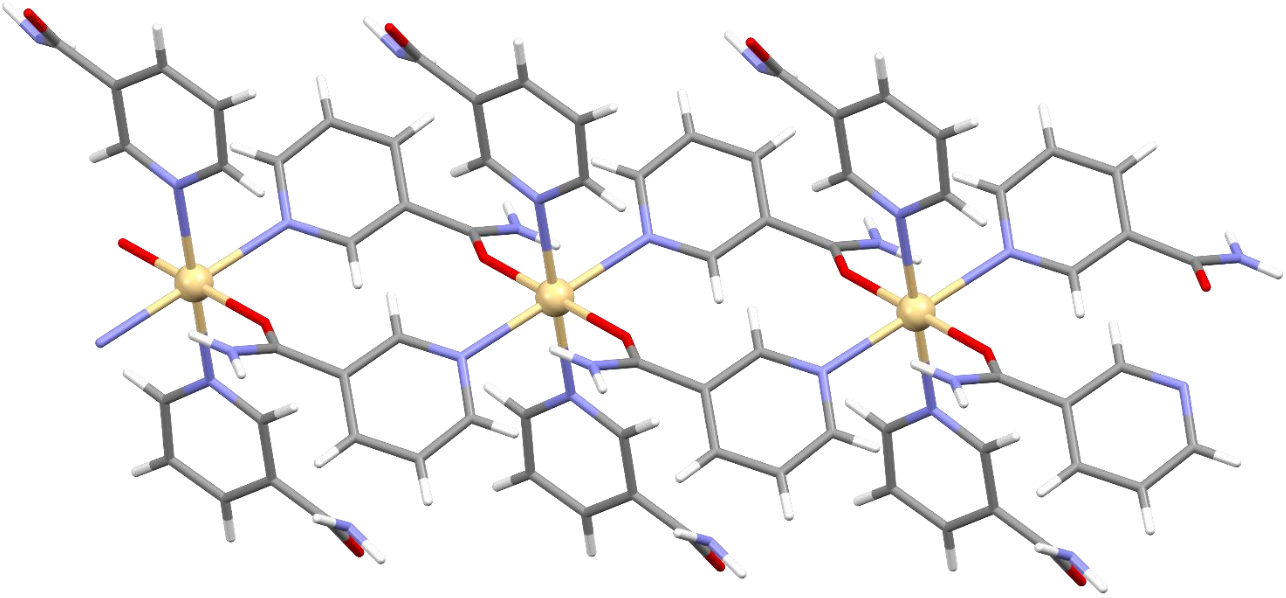

Figure 2. The infinite one-dimensional polymeric chain of {[Cd(nia)$_4$](ClO_4)$_2$}$_n$ (**2**) extending along the *a* crystallographic axis.

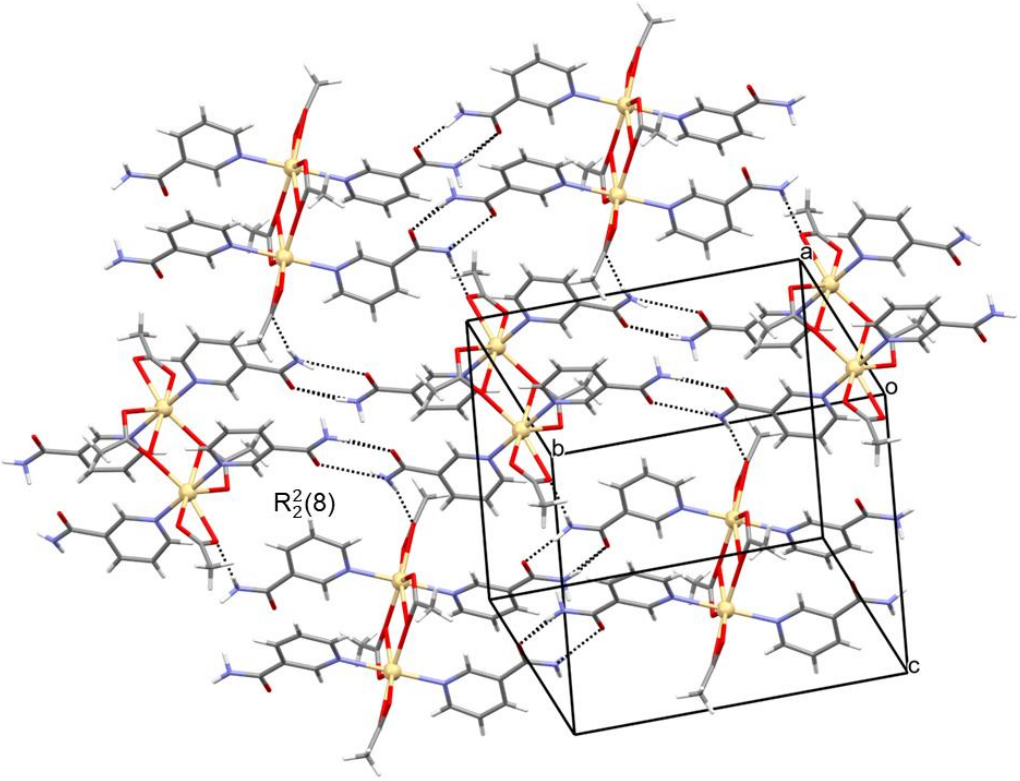

Figure 3. A fragment of the structure of [Cd(CH_3COO)$_2$(nia)$_2$]$_2$ (**1**), showing the centrosymmetric dimers of **1**, which are connected into a double chain via amide groups (the dimeric hydrogen-bond $R_2^2(8)$ motif within the chains is shown by dotted lines). These chains are in turn assembled by the N–H$\cdots$O hydrogen bonds.

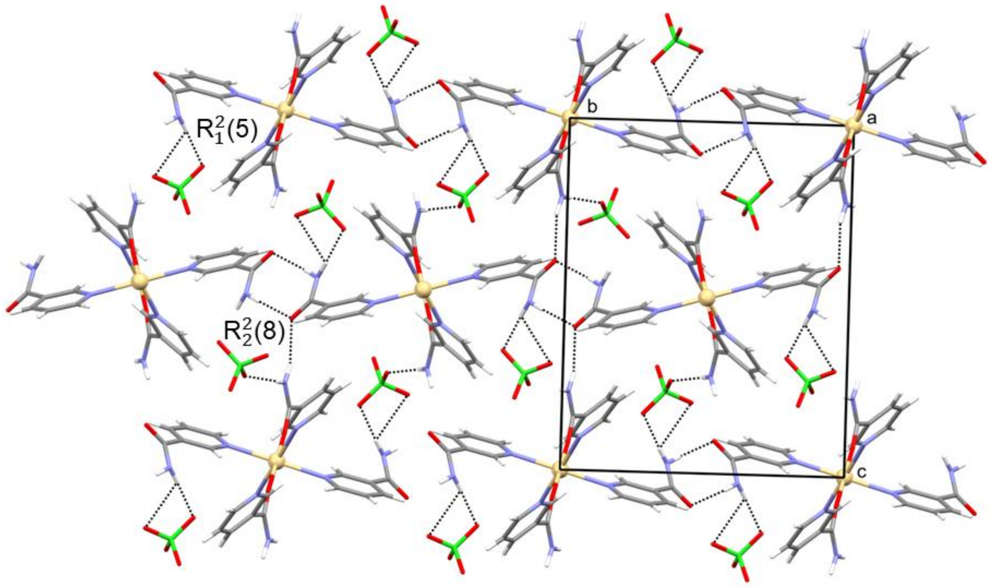

Figure 4. A view of the structure of $\{[Cd(nia)_4](ClO_4)_2\}_n$ (**2**) down the *a* crystallographic axis. The 1-D polymeric chains, represented as monomeric molecules in this projection, are linked into a chain via the amide groups along the *b* crystallographic axis. These chains and perchlorate ions are in turn assembled along the *c* crystallographic axis by the N–H· · · O hydrogen bonds (the dimeric hydrogen-bond $R_2^2(8)$ and $R_1^2(5)$ motifs are shown by dotted lines).

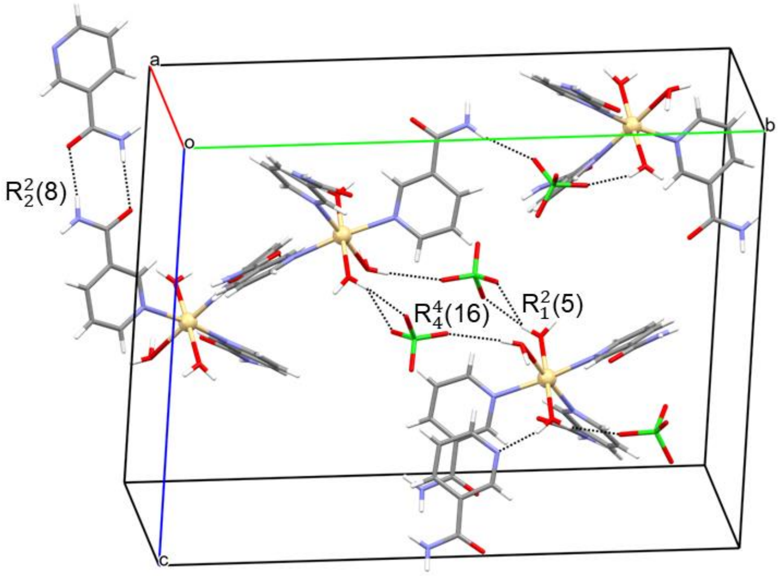

Figure 5. A fragment of the structure of $[Cd(H_2O)_3(nia)_3](ClO_4)_2$·nia (**3**), showing the dimeric hydrogen-bond $R_2^2(8)$ and $R_1^2(5)$ motifs and tetrameric hydrogen-bond $R_4^4(16)$ motif by dotted lines.

3.3. IR Spectra

The analysis of the IR spectra (Figure 6 and Figures S1–S3) was based on the data known from the literature for nia and its metal complexes [33–37]. The IR spectra of **1**–**3** show strong and broad absorptions of the antisymmetric (3400–3310 cm^{-1}) and symmetric (3270–3180 cm^{-1}) N–H stretching vibrations of the amide group. A more pronounced broadening of the amide stretching vibrations in the IR spectrum of **3** can be attributed to the overlapping with O–H stretching vibrations of the coordinated water molecules and to the strong O–H· · · O and O–H· · · N intermolecular hydrogen bonds. The characteristic strong C=O stretching bands of the amide group are observed at 1696 cm^{-1}, 1670 cm^{-1} (**1**), and at 1695 cm^{-1}, 1664 cm^{-1} (**3**). The position of the C=O stretching bands in the

IR spectrum of the uncoordinated nia is very similar (1699 cm^{-1}, 1670 cm^{-1}), suggesting the existence of uncoordinated amide groups. A significant negative shift of the carbonyl frequency observed at 1666 cm^{-1} in the IR spectrum of **2** is consistent with coordination of the bridging nia ligand via the carbonyl oxygen atom. The IR spectra of compounds **1**–**3** exhibit broad bands related to the vibrations of oxoanions [38]. Two bands centered at 1580 cm^{-1} and at 1418 in the IR spectrum of the **1** correspond to the antisymmetric and symmetric stretching vibrations of the acetate ions, respectively. The difference (Δ) between antisymmetric and symmetric stretching vibrations of the carboxylates can be used to distinguish ionic, unidentate, bidentate (chelating), and bridging carboxylate groups [38,39]. The calculated Δ value for compound **1** is 162 cm^{-1}, which is in good agreement with the values expected for bridging carboxylates. The intensive bands at 1143 cm^{-1}, 1113 cm^{-1}, and 1086 cm^{-1} and the weak band at 940 cm^{-1} are related to the vibrations of the uncoordinated perchlorate ion [11,38]. A significant broadening of the band in the 1150–1000 cm^{-1} region of the IR spectrum of **3** (centered at 1094 cm^{-1}) can be related to complex hydrogen bonding of uncoordinated perchlorate ions and cocrystallized nicotinamide molecules.

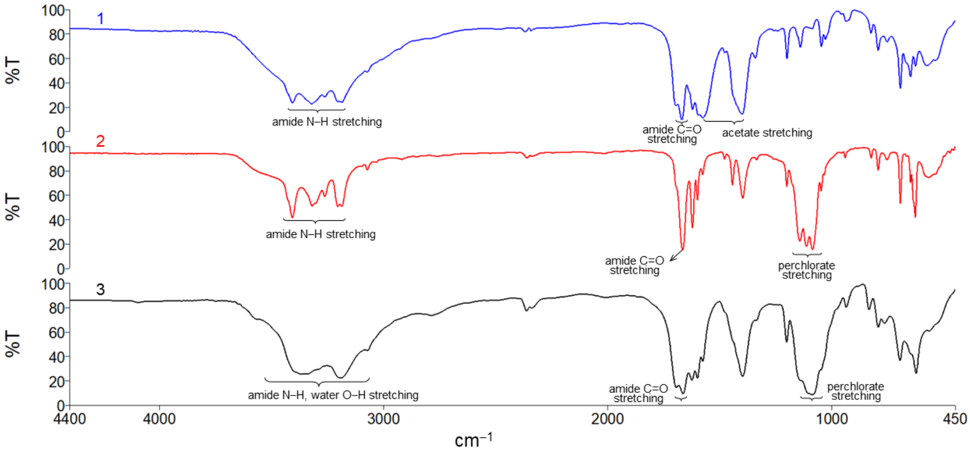

Figure 6. IR spectra of $[Cd(CH_3COO)_2(nia)_2]_2$ (**1**), $\{[Cd(nia)_4](ClO_4)_2\}_n$ (**2**), and $[Cd(H_2O)_3(nia)_3](ClO_4)_2 \cdot nia$ (**3**).

3.4. Thermal Properties

The thermal stability of the compounds was studied in flowing nitrogen by a TGA/DTA method (Figures 7 and S4–S6). Compound **1** is thermally stable up to 161 °C, followed by continuous thermal degradation. The total mass loss of 84.01% was observed at 500 °C. The thermal degradation of the compound is characterized by three endothermic signals (189, 241, and 276 °C) on the DTA curve. The TGA curve of the polymeric compound **2** reveals a two-step decomposition. The first step between 178 °C and 261 °C is accompanied by a 30.43% weight loss, which likely corresponds to the elimination of two nia molecules from the crystal structure (cal. 30.53%). In the temperature range from 261 °C to 500 °C, 55.88% of the initial mass is lost, which likely corresponds to the elimination of two nia ligands and two perchlorate anions (cal. 55.41%). The DTA curve of compound **2** reveals three broad signals: the endothermic at 219 °C and 306 °C, and the exothermic at 368 °C. The total mass loss of 86.31% was observed at 500 °C. The thermal decomposition of compound **3** starts with the elimination of three water molecules. The corresponding TGA curve shows a weight loss of 5.27% (cal. 5.62%). The elimination of water molecules is characterized by a broad endothermic signal at 114 °C, as observed on the DTA curve. The thermal degradation of an anhydrous compound starts at 165 °C, and the second step ends at 245 °C with a mass loss of 28.48%, which likely corresponds to the decomposition of two nia ligands (cal. 28.60%). The DTA curve reveals one broad endothermic signal at 218 °C. The third step of the thermal decomposition (weight loss of 49.66%, range 245 °C to 500 °C) likely corresponds to the elimination of two nia ligands and two perchlorate anions (cal. 51.90%). This step is characterized by one endothermic (310 °C) and one exothermic (349 °C) signal on the DTA curve. The total mass loss of 86.42% was observed at 500 °C.

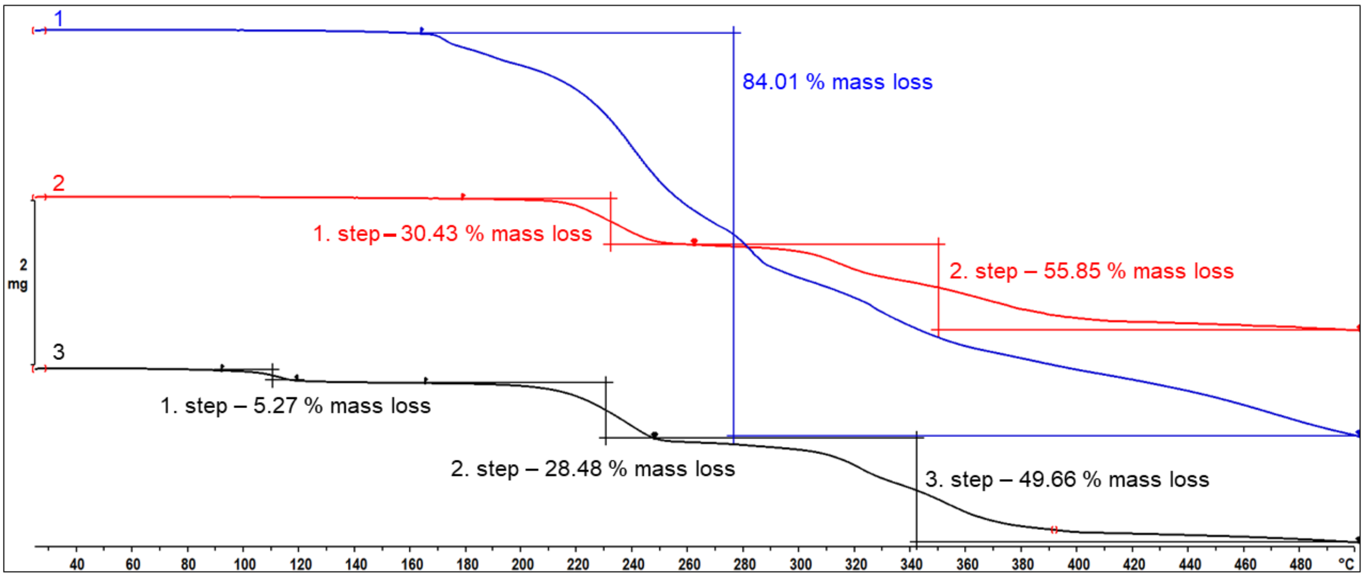

Figure 7. TGA curves of $[Cd(CH_3COO)_2(nia)_2]_2$ (**1**), $\{[Cd(nia)_4](ClO_4)_2\}_n$ (**2**), and $[Cd(H_2O)_3(nia)_3](ClO_4)_2\cdot nia$ (**3**).

4. Conclusions

The cadmium(II) coordination compounds with nicotinamide and acetate (**1**) or perchlorate (**2** and **3**) have been prepared. The cadmium(II) coordination environment can be modified by employing these anions, as it was found to be pentagonal-bipyramidal (high coordination number) in the presence of chelating and bridging acetate anions in **1** and octahedral in the presence of non-coordinating perchlorate anions in both **2** and **3**. Moreover, the full bridging capabilities of acetate ions were reflected in connecting the cadmium(II) ions into a dimer of **1**. Surprisingly, it was shown that the dimensionality of cadmium(II) complexes with nicotinamide and perchlorate depends upon the solvent used for the design of these compounds, while perchlorate anions remain uncoordinated in both cases. Nicotinamide ligands unexpectedly act as bridges between cadmium(II) ions in a 1-D coordination polymer of **2**, if isolated from an ethanol solution. On the contrary, nicotinamide ligands are bound monodentately to cadmium(II) ions in a discrete complex of **3** (as expected by analogy to isonicotinamide in zinc(II) complexes [11]) if isolated from an aqueous solution. It seems the water molecules compete with nicotinamide ligands for coordination to cadmium(II) ions (as in **3**), preventing the bridging ability of nicotinamide in aqueous solution. However, in the absence of water molecules (e.g., in an ethanol solution), the cadmium(II) ions are exclusively coordinated by nicotinamide ligands (as in **2**), enabling the bridging potential of nicotinamide.

Finally, the presence of either acetate or perchlorate anions does not disrupt the formation of the anticipated supramolecular amide-amide homosynthon $R^2_2(8)$, as it is preserved in the hydrogen-bonded frameworks of all the compounds. The dimensionality of the studied compounds also differs (dimer in **1**, polymer in **2**, and monomer in **3**), so the influence of these anions on homosynthon preservation/disruption cannot be directly compared or predicted.

The results of IR spectroscopy and TGA/DTA analysis are in a good agreement with the crystal structures of coordination compounds **1**–**3**.

Supplementary Materials: The following are available online at https://www.mdpi.com/article/10.3390/chemistry5020092/s1, Table S1: Selected bond lengths (Å) and angles (°) for $[Cd(CH_3COO)_2(nia)_2]_2$ (**1**), $\{[Cd(nia)_4](ClO_4)_2\}_n$ (**2**), and $[Cd(H_2O)_3(nia)_3](ClO_4)_2\cdot nia$ (**3**), Table S2: The hydrogen bond geometry for $[Cd(CH_3COO)_2(nia)_2]_2$ (**1**), $\{[Cd(nia)_4](ClO_4)_2\}_n$ (**2**), and $[Cd(H_2O)_3(nia)_3](ClO_4)_2\cdot nia$ (**3**), Figure S1: IR spectrum of $[Cd(CH_3COO)_2(nia)_2]_2$ (**1**), Figure S2: IR spectrum of $\{[Cd(nia)_4](ClO_4)_2\}_n$ (**2**), Figure S3: IR spectrum of $[Cd(H_2O)_3(nia)_3](ClO_4)_2\cdot nia$ (**3**), Figure S4: TGA/DTA curves of $[Cd(CH_3COO)_2(nia)_2]_2$ (**1**), Figure S5: TGA/DTA curves of $\{[Cd(nia)_4](ClO_4)_2\}_n$ (**2**), Figure S6: TGA/DTA curves of $[Cd(H_2O)_3(nia)_3](ClO_4)_2\cdot nia$ (**3**). Deposition numbers 2253343 for **1**, 2253344 for **2**, and 2253345 for **3** contain the supplementary crystallographic data for this paper. These data are provided free of charge by the joint Cambridge Crystallographic Data Centre and Fachinformationszentrum Karlsruhe Access Structures service at www.ccdc.cam.ac.uk/structures.

Author Contributions: Conceptualization, B.-M.K. and Ž.S.; methodology, Ž.S., B.-M.K., M.K. and M.Đ.; validation, B.-M.K. and Ž.S.; formal analysis, B.-M.K., Ž.S. and M.K.; investigation, B.-M.K., Ž.S., M.K. and Z.P.; resources, Z.P.; data curation, Ž.S. and M.Đ.; writing—original draft preparation, B.-M.K. and Ž.S.; writing—review and editing, B.-M.K., Ž.S., M.Đ. and Z.P.; visualization, B.-M.K. and Ž.S.; supervision, Ž.S.; project administration, Z.P.; funding acquisition, Z.P. All authors have read and agreed to the published version of the manuscript.

Funding: This research was funded by the University of Zagreb, Zagreb, Croatia (Grant No. 118120281106) and by the Ministry of Science, Education and Sports of the Republic of Croatia (Grant No. 119-1193079-1332). The APC was waived in full by the publisher.

Institutional Review Board Statement: Not applicable.

Informed Consent Statement: Not applicable.

Data Availability Statement: Not applicable.

Conflicts of Interest: The authors declare no conflict of interest. The funders had no role in the design of the study; in the collection, analyses, or interpretation of data; in the writing of the manuscript, or in the decision to publish the results.

References

1. Allendorf, M.D.; Bauer, C.A.; Bhakta, R.K.; Houk, R.J.T. Luminescent metal–organic frameworks. *Chem. Soc. Rev.* **2009**, *38*, 1330–1352. [CrossRef] [PubMed]
2. Cui, Y.; Yue, Y.; Qian, G.; Chen, B. Luminescent Functional Metal–Organic Frameworks. *Chem. Rev.* **2012**, *112*, 1126–1162. [CrossRef] [PubMed]
3. Zheng, S.-L.; Chen, X.-M. Recent Advances in Luminescent Monomeric, Multinuclear, and Polymeric Zn(II) and Cd(II) Coordination Complexes. *Aust. J. Chem.* **2004**, *57*, 703–712. [CrossRef]
4. Cepeda, J.; Rodríguez-Diéguez, A. Tuning the luminescence performance of metal–organic frameworks based on d^{10} metal ions: From an inherent versatile behaviour to their response to external stimuli. *CrystEngComm* **2016**, *18*, 8556–8573. [CrossRef]
5. Chisca, D.; Croitor, L.; Petuhov, O.; Kulikova, O.V.; Volodina, G.F.; Coropceanu, E.B.; Masunov, A.E.; Fonari, M.S. Tuning structures and emissive properties in a series of Zn(II) and Cd(II) coordination polymers containing dicarboxylic acids and nicotinamide pillars. *CrystEngComm* **2018**, *20*, 432–447. [CrossRef]
6. Mishra, A.; Gupta, R. Supramolecular architectures with pyridine-amide based ligands: Discrete molecular assemblies and their applications. *Dalton Trans.* **2014**, *43*, 7668–7682. [CrossRef]
7. Mukherjee, A. Building upon supramolecular synthons: Some aspects of crystal engineering. *Cryst. Growth Des.* **2015**, *15*, 3076–3085. [CrossRef]
8. Aakeröy, C.B.; Scott, B.M.T.; Desper, J. How robust is the hydrogen-bonded amide 'ladder' motif? *New J. Chem.* **2007**, *31*, 2044–2051. [CrossRef]
9. Bera, J.K.; Vo, T.-T.; Walton, R.A.; Dunbar, K.R. Hydrogen-bonding as a tool for building one-dimensional structures based on dimetal building blocks. *Polyhedron* **2003**, *22*, 3009–3014. [CrossRef]
10. Aakeröy, C.B. Supramolecular assembly of low-dimensional silver(I) architectures via amide–amide hydrogen bonds. *Chem. Comm.* **1998**, 1067–1068. [CrossRef]
11. Soldin, Ž.; Kukovec, B.-M.; Debač, T.; Đaković, M.; Popović, Z. Anion-assisted supramolecular assemblies of zinc(II) complexes with isonicotinamide. *Heliyon* **2022**, *8*, e09943. [CrossRef] [PubMed]
12. Zhao, J.; Yang, D.; Yang, X.-J.; Wu, B. Anion coordination chemistry: From recognition to supramolecular assembly. *Coord. Chem. Rev.* **2019**, *378*, 415–444. [CrossRef]
13. Đaković, M.; Jaźwiński, J.; Popović, Z. Impact of coordinated pseudohalide ions and picolinamide on supramolecular synthons in selected zinc and cadmium complexes. *Acta Chim. Slov.* **2015**, *62*, 328–336. [CrossRef] [PubMed]

14. Nezhadali Baghan, Z.; Salimi, A.; Eshtiagh-Hosseini, H.; Olive, A.G. Hydrogen-bonded 3D network of d^{10}-metal halide coordination polymer containing *N*-(3-pyridinyl) nicotinamide: Influence of ligand conformation, halide anions and solvent. *CrystEngComm* **2019**, *21*, 2691–2701. [CrossRef]
15. *CrysAlisPro*; Oxford Diffraction Ltd.: Yarnton, Oxfordshire, UK, 2010.
16. Sheldrick, G.M. *SHELXT*—Integrated space-group and crystal-structure determination. *Acta Crystallogr.* **2015**, *A71*, 3–8. [CrossRef]
17. Sheldrick, G.M. Crystal structure refinement with *SHELXL*. *Acta Crystallogr.* **2015**, *C71*, 3–8.
18. Macrae, C.F.; Sovago, I.; Cottrell, S.J.; Galek, P.T.A.; McCabe, P.; Pidcock, E.; Platings, M.; Shields, G.P.; Stevens, J.S.; Towler, M.; et al. *Mercury 4.0*: From visualization to analysis, design and prediction. *J. Appl. Crystallogr.* **2020**, *53*, 226–235. [CrossRef]
19. Groom, C.R.; Bruno, I.J.; Lightfoot, M.P.; Ward, S.C. The Cambridge Structural Database. *Acta Crystallogr.* **2016**, *B72*, 171–179. [CrossRef]
20. Bozkurt, N.; Dilek, N.; Çaylak Delibas, N.; Necefoglu, H.; Hökelek, T. Di-μ-nicotinamide-$\kappa^2 N^1:O:\kappa^2 O:N^1$-bis[aquabis(3-chloro benzoato- $\kappa^2 O,O'$)cadmium]. *Acta Crystallogr.* **2013**, *E69*, m389–m390.
21. Öztürkkan Özbeka, F.E.; Sertçelika, M.; Yüksekb, M.; Elmalıc, A.; Şahind, E. The superiority of the classical synthesis compared to the hydrothermal synthesis upon the structural, optical absorption and fluorescent properties of new Cd(II) 3-fluorobenzoate complexes with Pyridine-3-carboxamide/Pyridine-3-carboxylate. *Inorg. Chim. Acta* **2020**, *509*, 119694. [CrossRef]
22. Cakir, S.; Naumov, P.; Bulut, I.; Bicer, E.; Cakir, O.; Jovanovski, G.; Razak, I.A.; Chantrapromma, S.; Fun, H.-K.; Ng, S.W. Di aquabis(nicotinamide) bis(o-sulfobenzimidato-*N*) cadmium(II). *Acta Crystallogr.* **2001**, *E57*, m431–m432.
23. Dincel, Ö.; Tercan, B.; Çimen, E.; Necefoğlu, H.; Hökelek, T. Bis(μ-4-methyl benzoato)-$\kappa^3 O,O':O;\kappa^3 O:O,O'$-bis[aqua(4-methyl benzoato-$\kappa^2 O,O'$)(nicotinamide-κN^1)cadmium]. *Acta Crystallogr.* **2012**, *E68*, m1510–m1511.
24. Zhang, K.-L.; Yang, B.; Lin, J.-G.; Ng, S.W. *trans,trans,trans*-Diaquabis(nicotinamide κ*N*)bis (2-nitro benzoato κ*O*)cadmium(II) dihydrate. *Acta Crystallogr.* **2009**, *E65*, m292.
25. Hökelek, T.; Özkaya, S.; Necefoğlu, H. Crystal structure and Hirshfeld surface analysis of aquabis(nicotinamide-κN^1)bis(2,4,6-tri methyl benzoato-$\kappa^2 O,O'$)cadmium(II). *Acta Crystallogr.* **2018**, *E74*, 246–251.
26. Deng, Z.-P.; Gao, S.; Ng, S.W. Tetraaquabis(nicotinamide-κ*N*)cadmium(II) bis (4-formyl benzoate). *Acta Crystallogr.* **2007**, *E63*, m2323.
27. Çaylak Delibas, N.; Necefoglu, H.; Hökelek, T. Diaquabis(2-hydroxy benzoato- κO^1)bis (nicotinamide-κN^1)cadmium-diaquabis(2-hydroxy benzoato-$\kappa^2 O^1,O^{1\prime}$)(nicotinamide-κ*N*)cadmium-water (1/2/4). *Acta Crystallogr.* **2013**, *E69*, m191–m192.
28. Yang, G.; Zhu, H.-G.; Liang, B.-H.; Chen, X.-M. Syntheses and crystal structures of four metal–organic co-ordination networks constructed from cadmium(II) thiocyanate and nicotinic acid derivatives with hydrogen bonds. *J. Chem. Soc. Dalton Trans.* **2001**, 580–585. [CrossRef]
29. Hökelek, T.; Süzen, Y.; Tercan, B.; Aybirdi, Ö.; Necefoglu, H. Bis[μ-4-(dimethyl amino) benzoato]-$\kappa^3 O,O':O;\kappa^3 O:O,O'$-bis{aqua[4-(dimethyl amino) benzoato-$\kappa^2 O,O'$](nicotinamide-κN^1)cadmium(II)}. *Acta Crystallogr.* **2010**, *E66*, m782–m783.
30. Li, C.; Chen, M.; Shao, C. *trans*-Tetraaquabis(nicotinamide-κ*N*)cadmium(II) biphenyl-4,4′-disulfonate. *Acta Crystallogr.* **2008**, *E64*, m424. [CrossRef] [PubMed]
31. Hökelek, T.; Saglam, E.G.; Tercan, B.; Aybirdi, Ö.; Necefoglu, H. Bis[μ-4-(methyl amino) benzoato]-$\kappa^3 O,O':O$; $\kappa^3 O:O,O'$-bis{aqua[4-(methyl amino) benzoato-$\kappa^2 O,O'$](nicotinamide-κ*N*)cadmium(II)}. *Acta Crystallogr.* **2010**, *E66*, m1559–m1560.
32. Lian, Z.; Zhao, N.; Yang, F.; Liu, P. Crystal structure of *trans-trans-trans*-diaquabis(nicotinamide)-dinitratocadmium(II)–nicotinamide (1:2), $Cd(H_2O)_2(C_6H_6N_2O)_2(NO_3)_2 \cdot 2C_6H_6N_2O$. *Z. Kristallogr. NCS* **2011**, *226*, 289–290.
33. Ramalingam, S.; Periandy, S.; Govindarajan, M.; Mohan, S. FT-IR and FT-Raman vibrational spectra and molecular structure investigation of nicotinamide: A combined experimental and theoretical study. *Spectrochim. Acta A Mol. Biomol. Spectrosc.* **2010**, *75*, 1552–1558. [CrossRef] [PubMed]
34. Paşaoğlu, H.; Güven, S.; Heren, Z.; Büyükgüngör, O. Synthesis, spectroscopic and structural investigation of ZnI_2(nicotinamide)$_2$, ZnI_2(isonicotinamide)$_2$ and [Zn(H_2O)$_2$(picolinamide)$_2$]I_2. *J. Mol. Struct.* **2006**, *794*, 270–276. [CrossRef]
35. Bayarı, S.; Ataç, A.; Yurdakul, Ş. Coordination behaviour of nicotinamide: An infrared spectroscopic study. *J. Mol. Struct.* **2003**, *655*, 163–170. [CrossRef]
36. İde, S.; Ataç, A.; Yurdakul, Ş. Spectroscopic and structural studies on dichlorobis(nicotinamide)zinc(II). *J. Mol. Struct.* **2002**, *605*, 103–107. [CrossRef]
37. Dziewulska-Kułaczkowska, A.; Mazur, L.; Ferenc, W. Thermal, spectroscopic and structural studies of zinc(II) complex with nicotinamide. *J. Therm. Anal. Calorim.* **2009**, *96*, 255–260. [CrossRef]
38. Nakamoto, K. *Infrared and Raman Spectra of Inorganic and Coordination Compounds: Part B: Applications in Coordination, Organometallic, and Bioinorganic Chemistry*, 6th ed.; John Wiley & Sons, Inc.: Hoboken, NJ, USA, 2009; pp. 64–67, 86–88.
39. Deacon, G.B.; Phillips, R.J. Relationships between the carbon-oxygen stretching frequencies of carboxylato complexes and the type of carboxylate coordination. *Coord. Chem. Rev.* **1980**, *33*, 227–250. [CrossRef]